Available online at www.sciencedirect.com
ScienceDirect
Journal of the European Ceramic Society 31 (2011) 863–868
www.elsevier.com/locate/jeurceramsoc

Reactive consolidation of layered-ternary Ti_2AlN ceramics by spark plasma sintering of a Ti/AlN powder mixture

Yi Liu [a,b], Zhongqi Shi [a], Jiping Wang [a], Guanjun Qiao [a], Zhihao Jin [a], Zhijian Shen [b,*]

[a] *State Key Laboratory for Mechanical Behavior of Materials, Xi'an Jiaotong University, 710049 Xi'an, PR China*
[b] *Department of Materials and Environmental Chemistry, Arrhenius Laboratory, Stockholm University, S-10691 Stockholm, Sweden*

Received 6 September 2010; received in revised form 3 November 2010; accepted 21 November 2010
Available online 14 December 2010

Abstract

A reactive consolidation process for preparing ternary Ti_2AlN ceramics was investigated by spark plasma sintering (SPS). A Ti/AlN powder mixture with a molar ratio of 2:1 was consolidated at temperatures ranging from 800 to 1450 °C. The phase composition and microstructure evolution during the process were characterized by X-ray diffraction (XRD) and scanning electron microscopy (SEM) equipped with an energy dispersive spectroscopy (EDS). A series of intermediate phases, namely TiN, Ti_3Al, Ti_3AlN and TiAl were indentified, which revealed a reaction pathway towards the formation of Ti_2AlN.

Keywords: Powders-solid state reaction; Sintering; Hot pressing; Nitrides; Electron microscopy

1. Introduction

Ti_2AlN belongs to a class of ternary ceramics with the general formula $M_{n+1}AX_n$ (where n is 1, 2 or 3, M is an early transition metal, A is an A-group element, and X is either C or N). It displays a unique combination of metallic and ceramic properties because of the layered structure of the compound and the intrinsic nature of the chemical bonding in Ti_2AlN.[1,4] For example, this material demonstrates metal-like properties, such as low hardness, high electrical and thermal conductivity, good machinability, thermal shock resistance and damage tolerance.[2] On the other hand, like other ceramics, it has relatively low density, high elastic modulus, high yield strength and significant plasticity at high temperature.[3] Therefore, it has been recognized as a candidate for many high-temperature applications.

Ti_2AlN was first discovered in 1963 by Jeitschko et al.[5] However, little progress was made until 1997. In a series of articles in the late 1990s, Barsoum et al. reported some of the properties of bulk Ti_2AlN ceramics.[1–3] In that work, a polycrystalline bulk Ti_2AlN ceramic was synthesized by hot isostatic pressing a mixture of Ti and AlN powders at 1600 °C for 4 h, or at 1400 °C for 48 h. The final product always contained 10–15 vol.% of extraneous phases even under optimized processing condition. Later, Jordan and Thadhani reported that Ti_2AlN can be fabricated by shock-activated reaction synthesis using Ti and AlN powders as precursors. Yet, it was noticed that a secondary phase, TiN, was hard to avoid.[6] In neither work was the reaction pathway from reactants to product so well investigated that the formation of extraneous phases could be explained. Recently, the successes in fabrication of dense and single-phase bulk Ti_2AlN ceramics by hot pressing of a mixture of Ti, TiN and Al powders have been reported.[7,8] Compared to Barsoum's work, hot-pressing achieved better mechanical properties while applying a shorter sintering time. Meanwhile, the single-phase bulk Ti_2AlN ceramics were prepared via the same reaction path by Yan et al. at 1200 °C for 10 min by spark plasma sintering (SPS).[9] This study demonstrated the potential for preparing of Ti_2AlN ceramics at even lower sintering temperature with shorter soaking time.

Over the last decades, spark plasma sintering (SPS), also known as pulsed electric current sintering (PECS), has been extensively used for synthesizing or consolidating various materials. It has been demonstrated that the high heating rate (up to 1000 °C/min) and the use of electric current or electric field can enhance the consolidation and reactive sintering of materials.[10–13] Indeed, many $M_{n+1}AX_n$ phases, such as Ti_3SiC_2, Ti_3AlC_2, Ti_2AlC and Cr_2AlC, have been successfully synthe-

* Corresponding author. Tel.: +46 8 16 2388; fax: +46 8 15 2187.
E-mail address: shen@mmk.su.se (Z. Shen).

0955-2219/$ – see front matter © 2010 Elsevier Ltd. All rights reserved.
doi:10.1016/j.jeurceramsoc.2010.11.018

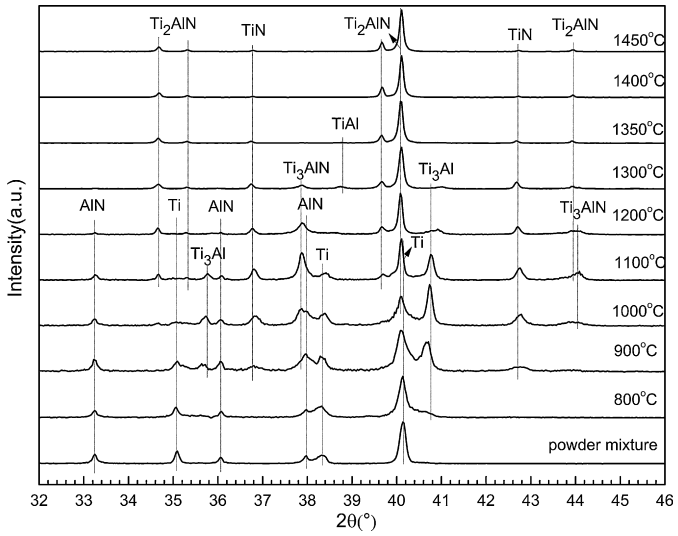

Fig. 1. XRD patterns recorded on the surfaces of bulk samples reactive consolidated at temperatures ranging from 800 to 1450 °C. Note that the theoretical position of the various (*h k l*) peaks related to the different phases is pointed out using dotted lines.

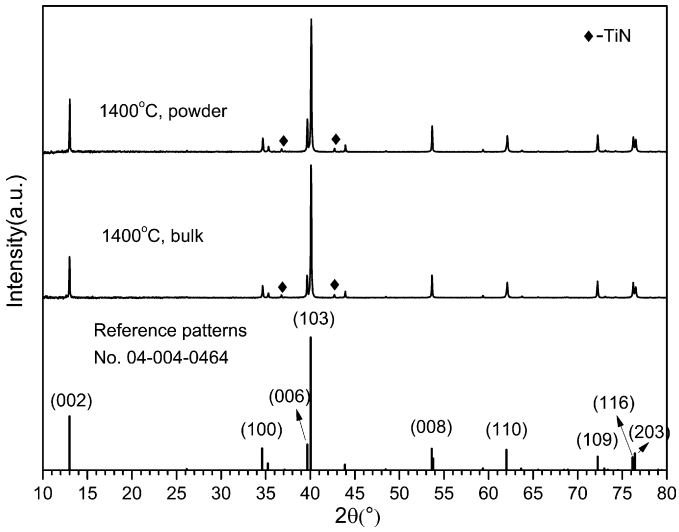

Fig. 2. Comparison of XRD patterns consolidated at 1400 °C.

sized by the SPS method.[14–18] However, so far there has been no report on the synthesis of Ti_2AlN by spark plasma sintering of a Ti/AlN powder mixture.

It is the aim of this work to fabricate fully dense and single-phase Ti_2AlN ceramics by spark plasma sintering of Ti/AlN powder mixtures. For better understanding of the mechanism of Ti_2AlN formation, the microstructure evolution and the reaction pathways during spark plasma sintering have been explored.

2. Experimental procedure

Powders of Ti (particle size: 400 mesh; purity: 99.5%) and AlN (particle size: 0.8 μm; purity: 99.2%) were used as precursors. The powder mixtures, having a stoichiometric Ti to AlN molar ratio of 2:1, were ball-milled for 12 h in an air-sealed container with a ball to powder mass ratio of 4:1. The powder mixtures were then dried, sieved (100 mesh) and filled into a graphite die with a length of 40 mm and inner and outer diameters of 12 mm and 40 mm, respectively. The subsequent spark plasma sintering was carried out in vacuum in a Dr. Sinter 2050 apparatus (Sumitomo Coal Mining Co., Japan). A heating rate of 100 °C/min and a uniaxial pressure of 50 MPa were applied. The temperature was regulated and controlled by an infrared pyrometer that was focused on the surface of the graphite die. The sintering temperatures were set in the range of 800–1450 °C, with a holding time of 5 min. After sintering, the surfaces of the samples were ground down 1 mm in order to eliminate the graphite contamination.

Bulk samples were directly used for X-ray diffraction (XRD) analysis to identify the phase constitution. The XRD patterns were recorded with a PANnalytical X'Pert, using Cu Kα1 radiation at 45 kV and 40 mA. A sample was also pulverised and checked by X-ray powder diffraction to verify the possible existence of grain orientation or texture. The microstructure was observed by Field Emission Gun Scanning Electron Microscopy (FE-SEM, JSM-7000F, JEOL, Tokyo, Japan) equipped with an energy dispersive spectroscopy (EDS) detector. Samples for the EDS analysis were polished down to 1 μm, finishing by diamond paste, and then etched in an acidic solution with HNO_3:HF:H_2O = 1:1:2.

3. Experimental results

3.1. Phase assemblages

Fig. 1 shows the XRD patterns of the samples SPS consolidated at temperatures ranging from 800 to 1450 °C for 5 min. In this figure, the emergence and disappearance of different phases are pointed out by the dotted lines which correspond to the theoretical position of the peaks. It can be seen that four intermediate phases, indicated as TiN, Ti_3Al, Ti_3AlN and TiAl, were detected

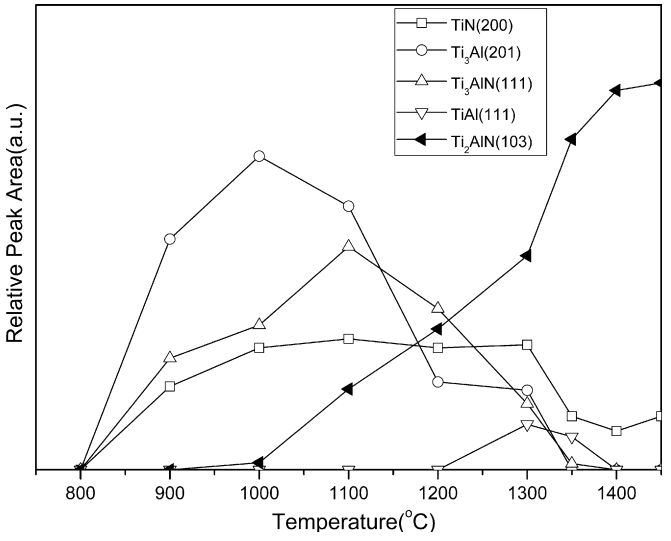

Fig. 3. The reaction sequence revealed by the XRD peak areas plotted versus the sintering temperature.

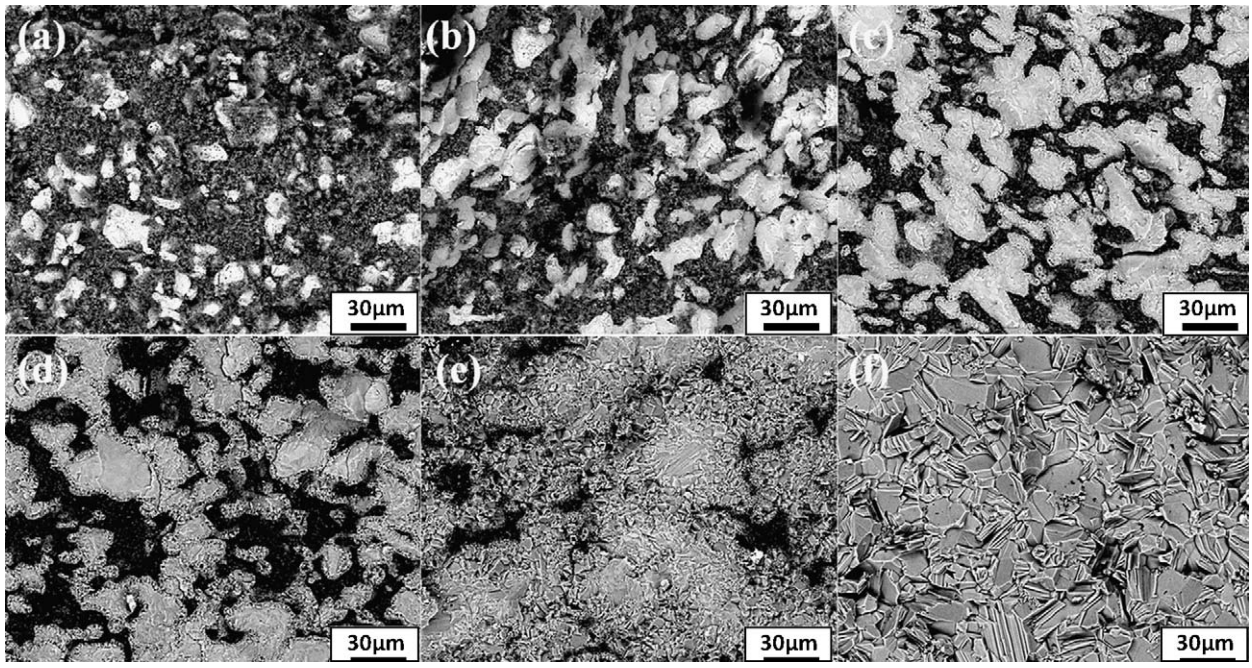

Fig. 4. Back-scattered SEM images of the fracture surface of the samples reactive consolidated at different temperatures for 5 min: (a) 900 °C, (b) 1000 °C, (c) 1100 °C, (d) 1200 °C, (e) 1300 °C and (f) 1400 °C.

during the formation of the targeted phase, Ti_2AlN. In addition, the peaks of Ti, Ti_3Al and TiN exhibited a slight offset from the theoretical position with the increase of the sintering temperature. When the temperature reached 1400 °C, all intermediate phases except TiN disappeared. A trace of TiN was still present even after sintering at 1450 °C. Both powder and bulk X-ray diffraction patterns show a perfect match with the reference patterns, as illustrated in Fig. 2. It was thus concluded that there was no apparent texture or oriented grain growth during the reactive consolidation process. To simplify the discussion below, all the phase analyses were based on the bulk X-ray diffractions.

It is hard to quantify different intermediate phases, due to their large number and small quantities. However, as mentioned above, since there is no texture in the sample, a qualitative estimate of the evolution of various phase contents can be deduced from the areas of the main diffraction peaks. As shown in Fig. 3, the intermediate phases, TiN, Ti_3Al and Ti_3AlN, emerged at 900 °C and increased in quantity up to 1000 °C, where the formation of a trace of Ti_2AlN phase was detected. From 1100 to 1300 °C, with increasing sintering temperature the contents of Ti_3Al and Ti_3AlN decreased whereas the content of Ti_2AlN phase increased. Surprisingly, the TiN phase content remained relatively stable in this temperature interval. In addition, the TiAl phase was also detected at 1300 °C. From 1300 to 1350 °C, the contents of the TiN, Ti_3Al and Ti_3AlN phases decreased drastically, whereas the content of Ti_2AlN exhibited a rapid increase. After reactive consolidation at 1350 °C, only a trace of Ti_3Al and Ti_3AlN phases could be detected, but there was still some TiN and TiAl phase left. When the temperature reached 1400 °C, all the intermediate phases except TiN disappeared.

3.2. Microstructure evolution

Fig. 4 shows back-scattered electron microscopic images taken on the fracture surfaces of samples reactively consolidated at various temperatures for 5 min. The corresponding EDS results showed that the dark areas are composed of small AlN particles. It is evident that the amount of AlN decreased with increasing sintering temperature. The AlN particles appear as voids in solid-state sintering: at low temperature, the white Ti particles were separated by dark AlN particles, corresponding to the initial stage in solid-state sintering. As the temperature increased from 900 to 1100 °C, the AlN content decreased, but the particles were still connected during pore elimination in the second sintering stage. When the temperature was increased above 1100 °C, the AlN particles became isolated and their content decreased continuously until disappearing at 1400 °C. This process is similar to the pore elimination taking place in the last stage of solid-state sintering.

Compared to AlN, the evolution of the Ti particles exhibited a more complicated behaviour during the reactive consolidation. The EDS analysis indicated that the white area is mainly composed of Ti at 900 °C, as seen in Fig. 4(a). With increasing sintering temperature, the composition of the white particles became more complicated. A continuous diffusion layer of N and Al was detected around the Ti particles. However, as illustrated in Fig. 4(b)–(d), it became difficult to verify the phase composition from the EDS analysis due to the deformation and connection of the white particles. Rapid grain growth and the formation of layer-structured grains occurred above 1300 °C. EDS analysis revealed that the layer-structured grains were Ti_2AlN, among which the small aggregated particles were found to be the residual TiN. Fig. 5 shows the microstructure of a coarse-

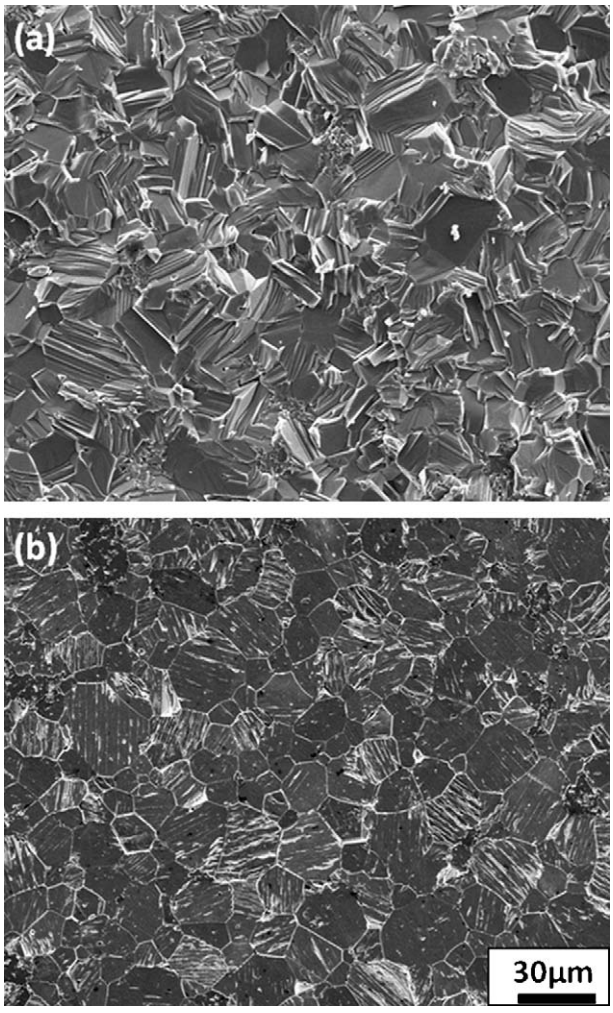

Fig. 5. Secondary SEM image of a sample sintered at 1400 °C for 5 min: (a) fractured and (b) polished and etched section.

grained sample with a mean grain size of ~25 μm and the highest Ti_2AlN content obtained by reactive consolidation at 1400 °C for 5 min. What appears evident is the uniform and equiaxed morphology of Ti_2AlN grains and their layered-grain structural character.

4. Discussion

4.1. The reaction sequences

4.1.1. Reactions taking place below 1000 °C

As seen in Fig. 1, no other phases except Ti and AlN can be detected at 800 °C by XRD, indicating that the reaction between Ti and AlN was negligible below 800 °C. When temperature reached 900 °C, the TiN, Ti_3Al and Ti_3AlN phases were formed, indicating that the reaction between Ti and AlN in this work was initiated between 800 °C and 900 °C. Once the reaction started, the TiN phase was first formed at the Ti/AlN interface, most probably by following reaction:

$$Ti + AlN \rightarrow TiN + Al \quad (1)$$

As per Eq. (1) Al is released when TiN is formed. Since the solubility of Al in TiN is rather limited, the released Al cannot dissolve in the TiN phase but diffuses through it and into the Ti particles. When Al atoms diffuse into Ti, a Ti-rich Ti–Al diffusion layer is formed between the TiN layer and the Ti particle. This diffusion layer may be composed of Ti_3Al and Ti (Al) solid solution according to the Ti–Al binary diagram and the XRD patterns.[19] It is worth noting that the Ti_3Al and Ti (Al) solid solutions have nonstoichiometric compositions. The content of Al in the Ti_3Al and Ti (Al) solid solutions changed gradually during the diffusion process, as indicated by a small offset of their XRD peaks. Likewise, TiN also has a nonstoichiometric composition, and the peaks of the corresponding XRD pattern also displayed a shift. When Ti_3Al phase is formed between the TiN layer and the Ti particles, the N atoms in the TiN phase immediately diffuse into Ti_3Al and thus form Ti_3AlN. This diffusion process can be described by the following equations:

$$3Ti + Al \rightarrow Ti_3Al \quad (2)$$

$$Ti_3Al + N \rightarrow Ti_3AlN \quad (3)$$

4.1.2. Reactions taking place between 1000 °C to 1300 °C

According to the Ti–N binary diagram,[20] the TiN phase is stable with a N content in a range of 37–50 at.% at 1000 °C. When the N atoms from AlN diffuse into the TiN layer, TiN becomes saturated with N, making TiN a rather stable phase as revealed by Fig. 3. When the N atoms in the TiN layer diffuse into Ti_3Al and form Ti_3AlN, the equilibrium is broken, however, and the N atoms in the TiN layer diffuse towards the Ti_3Al side. As a result, TiN shows a low N concentration on the AlN side, making the N atoms in AlN diffuse continuously into TiN. At the same time, the released Al diffuses through TiN and goes into the Ti_3AlN. When enough N and Al atoms diffuse into Ti_3AlN, then Ti_2AlN is formed between TiN and Ti_3AlN. Such a diffusion process can be described by the following equation:

$$2Ti_3Al + Al + N \rightarrow 3Ti_2AlN \quad (4)$$

After the formation of Ti_2AlN, a continuous reaction zone is established around the Ti particle. As shown in Fig. 6, it is composed of TiN, Ti_2AlN, Ti_3AlN and Ti_3Al from the outside to the inside of the Ti particle (as indicated by B, C, D and E, respectively in Fig. 6(b)). At increased temperatures, AlN continuously diffuses into the Ti particles, and as a consequence the diffusion layers move towards the centre of the Ti particle until all the Ti is consumed. In this temperature interval the reactions (1)–(4) take place simultaneously, resulting in a gradual increase of Ti_2AlN and decrease of AlN, Ti, Ti_3Al and Ti_3AlN. It is worth mentioning that the Ti_3Al phase disappears above 1200 °C, where it converts to Ti (Al) solid solution, and then re-transforms into Ti_3Al phase upon cooling.

4.1.3. Reactions taking place between 1300 °C and 1450 °C

When the temperature is further increased to 1300 °C, the amount of Ti_2AlN phase increases according to the reactions (1)–(4) until all the AlN is consumed. Meanwhile, the excess Al atoms diffused into Ti_3Al, encouraging the formation of

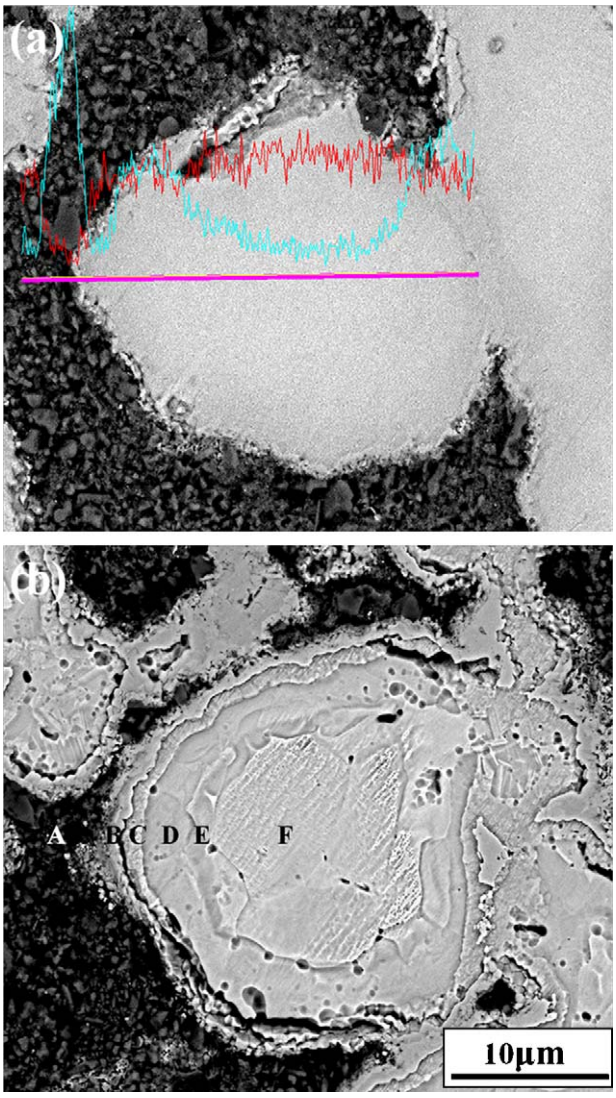

Fig. 6. SEM/EDS analysis of the samples sintered at 1200 °C. (a) Line scanning over a polished single particle, where the red and blue curves indicate the element distribution of Ti and Al, respectively and (b) polished and etched surface showing the formation of different layers around the Ti particle (A: AlN; B: TiN; C: Ti_2AlN; D: Ti_3AlN; E: Ti_3Al; F: Ti). (For interpretation of the references to color in the figure caption, the reader is referred to the web version of the article.)

a layer of TiAl between Ti_3Al and Ti_3AlN. The intermetallic compound TiAl becomes soft and deforms easily at elevated temperature under pressure. When TiN comes into contact with deformed TiAl, the Ti_2AlN phase forms in the following ways:

$$Ti_3Al + 2Al \rightarrow 3TiAl \quad (5)$$

$$TiN + TiAl \rightarrow Ti_2AlN \quad (6)$$

Reaction (6) is a crucial step in achieving high-purity Ti_2AlN. As mentioned above, the formation of Ti_2AlN below 1300 °C is mainly based on the diffusion of Al and N atoms. The role of TiN is to transfer Al and N from one side to the other. Once AlN is consumed and Ti_3AlN transforms to Ti_2AlN according to reactions (1)–(5), the diffusion rate decreases. TiN and TiAl,

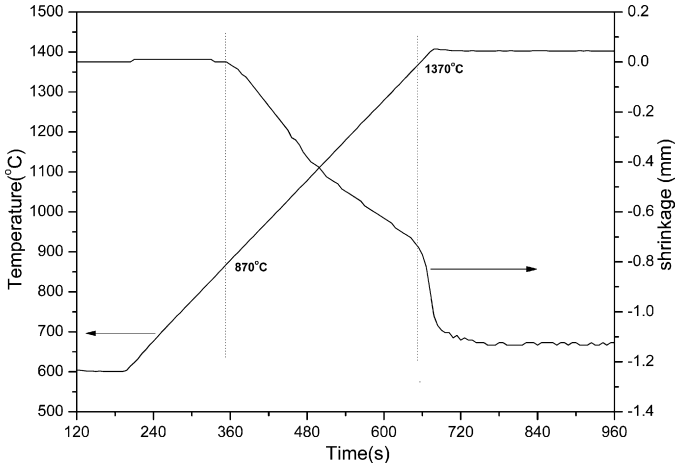

Fig. 7. The real-time shrinkage plotted versus temperature.

separated by the Ti_2AlN particles, remain and coexist according to the Ti–Al–N ternary diagram.[20] This may be the reason why it was hard to obtain high-purity Ti_2AlN in Barsoum's work.[1–3]

4.2. The characters of reactive consolidation performed by spark plasma sintering

Since all the intermediate phases, such as TiN, Ti_3AlN, Ti_3Al and TiAl, and the target phase Ti_2AlN are electrically conductive, the pulse current passes through the sintering compact when the percolation is established. It is thus expected that the local heating along the conductive network will promote diffusion and enhance densification. Besides, during SPS the applied uniaxial pressure of 50 MPa results in a shear stress between particles during densification. Therefore, the soft materials, such as Ti, Ti_3Al and TiAl are easily deformed, as seen in Fig. 4. As a consequence, the continuous diffusion layer is easily broken, promoting further diffusion. Especially above 1350 °C, the deformation of TiAl enhances the possibility for it to contact and react with TiN to form Ti_2AlN.

To better understand the reaction between TiAl and TiN it is worthwhile examining the real-time sintering curve, as shown in Fig. 7. Apparently, the first shrinkage is initiated already at 870 °C, which corresponds to the beginning of reactions (1) and (2). The second shrinkage, occurring at 1370 °C with radically increased speed, is essential. It may indicate the melting of TiAl. According to the Ti–Al diagram,[19] the TiAl alloy melts at 1445 °C, which is 75 °C higher than the apparent SPS processing temperature, 1370 °C. It is well known that there exists a temperature difference between the sample inside the graphite die and the die surface as recorded by a pyrometer focused on the surface. Such a temperature gradient may be more than 100 °C when a conductive sample is concerned.[21–23] Once TiAl melts, the melt easily flows through the structural voids and gets into contact with TiN, thus forming Ti_2AlN. On the other hand, the TiAl melt is also easily squeezed out of the pressing die under the applied uniaxial pressure. This loss of TiAl may explain why there is always a small amount of TiN remaining in the final prod-

uct. Therefore, optimum sintering parameters for avoiding the escape of TiAl should be explored in order to get a single-phase Ti_2AlN ceramic. Besides, the conditions for homogeneous mixing of starting reactant powders with fine particle sizes should also be investigated. In this regard, it is of great importance to use fine Ti powders, as it is the size of Ti particles that determines the diffusion distance.

4.3. SPS versus HIP

As discussed above, one obvious advantage of SPS is the shear stress built up on each individual particle during the process, which breaks the reactive layers and stimulates further diffusion. In early work performed by Barsoum,[1–3] a hot isostatic pressing method was used. Under this processing condition, although an isostatic compressive stress was applied to each individual reactant particle, it did not facilitate breaking of the diffusion layers. Another advantage of SPS originates from the enhanced diffusion. During the conventional heating processes, the diffusion between Ti and AlN is rather limited.[24] By employing the SPS process, the diffusion processes have been obviously enhanced, as in this work a high purity Ti_2AlN ceramic with a minimum of TiN has been fabricated with an annealing time of only 5 min. This may be attributed to the strong current passing through the conductive sample and the high heating rate achieved. At this stage it is, however, hard to say which one dominates the contribution, as these two factors are always linked together. Further work is required to distinguish between these two effects.

5. Conclusions

The Ti_2AlN ceramic was prepared by SPS of a Ti/AlN powder mixture with a holding time of 5 min. The final microstructure was composed of uniform and equiaxed grains with a mean particle size of $\sim$25 μm. The reaction path was revealed by investigating the phase composition and microstructure evolution which indicated that the reaction between Ti and AlN was a process of AlN diffusing into Ti. It was also found that this kind of reaction was obviously enhanced by the SPS technique.

Acknowledgements

This work has been partially supported by the Swedish Research Council (VR) through its Research Link program. SEM studies were performed at the Arrhenius Laboratory Electron Microscopy Centre, which is supported by the Knut and Alice Wallenberg foundation. The authors acknowledge the technical support of Kjell Jansson and Yan Xiong in SEM observation. Y. Liu acknowledges the financial support of the graduate school of Xi'an Jiaotong University for his stay at Stockholm University as an exchange student.

References

1. Barsoum MW. The M_{N+1} AXN phases: a new class of solids; thermodynamically stable nanolaminates. *Prog Solid State Chem* 2000;**28**:201–81.
2. Barsoum MW, Ali M, El-Raghy T. Processing and characterization of Ti_2AlC, Ti_2AlN, and $Ti_2AlC_{0.5}N_{0.5}$. *Metall Mater Trans A* 2000;**31**:1857–65.
3. Barsoum MW, Brodkin D, El-Raghy T. Layered machinable ceramics for high temperature applications. *Scr Mater* 1997;**36**:535–41.
4. Zhou YC, Sun ZM. Electronic structure and bonding properties of layered machinable Ti_2AlC and Ti_2AlN ceramics. *Phys Rev B* 2000;**61**:12570–3.
5. Jeitschko W, Nowotny H, Benesovsky F. Ti_2AlN, eine stickstoffhaltige H-phase. *Monatsh Chem* 1963;**94**:1198–200.
6. Jordan JL, Thadhani NN. Effect of shock-activation on post-shock reaction synthesis of ternary ceramics. *AIP Conf Proc* 2002;**620**:1097–100.
7. Lin ZJ, Zhuo MJ, Li MS, Wang JY, Zhou YC. Synthesis and microstructure of layered-ternary Ti_2AlN ceramic. *Scr Mater* 2007;**56**:1115–8.
8. Hashimoto H, Sun ZM. An approach to the synthesis of AlN–Ti_2AlN composite. *J Jpn Soc Powder Metall* 2009;**56**:541–5.
9. Yan M, Mei BC, Zhu JQ, Tian CG, Wang P. Synthesis of high-purity bulk Ti_2AlN by spark plasma sintering (SPS). *Ceram Int* 2008;**34**:1439–42.
10. Shen ZJ, Zhao Z, Peng H, Nygren M. Formation of tough interlocking microstructures in silicon nitride ceramics by dynamic ripening. *Nature* 2002;**417**:266–9.
11. Olevsky EA, Kandukuri S, Froyen L. Consolidation enhancement in spark-plasma sintering: impact of high heating rates. *J Appl Phys* 2007;**102**:114913.
12. Munir ZA, Anselmi-Tamburini U, Ohyanagi M. The effect of electric field and pressure on the synthesis and consolidation of materials: a review of the spark plasma sintering method. *J Mater Sci* 2006;**41**:763–77.
13. Anselmi-Tamburini U, Garay JE, Munir ZA. Fundamental investigations on the spark plasma sintering/synthesis process. III. Current effect on reactivity. *Mater Sci Eng A* 2005;**407**:24–30.
14. Zhang ZF, Sun ZM, Hashimoto H, Abe T. Application of pulse discharge sintering (PDS) technique to rapid synthesis of Ti_3SiC_2 from Ti/Si/C powders. *J Eur Ceram Soc* 2002;**22**:2957–61.
15. Zou Y, Sun ZM, Hashimoto H, Tada S. Synthesis of high-purity polycrystalline Ti_3AlC_2 through pulse discharge sintering Ti/Al/TiC powders. *J Alloys Compd* 2008;**456**:456–60.
16. Zou Y, Sun ZM, Tada S, Hashimoto H. Synthesis reactions for Ti_3AlC_2 through pulse discharge sintering Ti/Al_4C_3/TiC powder mixture. *Scr Mater* 2006;**55**:767–70.
17. Zhou WB, Mei BC, Zhu JQ, Hong XL. Rapid synthesis of Ti_2AlC by spark plasma sintering technique. *Mater Lett* 2005;**59**:131–4.
18. Tian WB, Vanmeensel K, Wang PL, Zhang GJ, Li YX, Vleugels J, et al. Synthesis and characterization of Cr_2AlC ceramics prepared by spark plasma sintering. *Matter Lett* 2007;**61**:4442–5.
19. Ohnuma I, Fujita Y, Mitsui H, Ishikawa K, Kainuma R, Ishida K. Phase equilibria in the Ti–Al binary system. *Acta Mater* 2000;**48**:3113–23.
20. Han YS, Kalmykov KB, Dunaev SF, Zaitsev AI. Solid-state phase equilibria in the titanium–aluminum–nitrogen system. *J Phase Equilib Diff* 2004;**25**:427–36.
21. Eriksson M, Shen Z, Nygren M. Fast densification and deformation of titanium powder. *Powder Metall* 2005;**48**:231–6.
22. Anselmi-Tamburini U, Gennari S, Garay JE, Munir ZA. Fundamental investigations on the spark plasma sintering/synthesis process. II. Modeling of current and temperature distributions. *Mater Sci Eng A* 2005;**394**:139–48.
23. Vanmeensel K, Laptev A, Hennicke J, Vleugels J, Van der Biest O. Modelling of the temperature distribution during field assisted sintering. *Acta Mater* 2005;**53**:4379–88.
24. Chiu CH, Lin CC. Microstructural characterization and phase development at the interface between aluminum nitride and titanium after annealing at 1300–1500 °C. *J Am Ceram Soc* 2006;**89**:1409–18.